DOI: 10.18462/iir.icr.2023.0422

Integration of Cold Thermal Energy Storage at a Pelagic Fish Processing Plant: A Modelling Approach

Eirik Starheim SVENDSEN*[(a)], Jan BENGSCH[(a)], Kristina Norne WIDELL[(a)], Håkon SELVNES[(b)], Alexis SEVAULT[(b)], Armin HAFNER[(c)], Tom Ståle NORDTVEDT[(a)]

[(a)] SINTEF Ocean
7465 Trondheim, Norway
[(b)] SINTEF Energy Research
7465 Trondheim, Norway
[(c)] Norwegian University of Science and Technology, Dep. Of Energy and Process Engineering
N-7491 Trondheim, Norway
*Corresponding author: eirik.starheim.svendsen@sintef.no

ABSTRACT

Energy intensive sectors such as food processing are paying more and more attention towards energy conservation and reducing their total carbon footprint. The energy demand of a pelagic fish processing plant has been evaluated in a previous study, including an initial evaluation of how a cold thermal energy storage (CTES) system can be implemented and its advantages. Results of the analysis showed that the energy demand followed a seasonal cycle linked to the availability of raw material; the refrigeration systems accounted for approximately 75 % of the total energy demand and there could be a large potential if implementing a CTES system using phase change material (PCM) as the storage medium for diurnal charging/discharging cycles. In the current paper, the previous study is continued by investigating and quantifying the effects of implementing a CTES system on the low-temperature (-40 °C) refrigeration circuit. A dynamic model of the current refrigeration system was built in the Modelica/Dymola environment, including a modified version with CTES integration. Subsequent simulations were performed with varying storage dimensions. The model of the CTES component was based on a pillow-plate heat exchanger unit, previously validated with experimental data. The results revealed a potential for reducing peaks in the power consumption and an increased flexibility with regards to management of the thermal energy demand. Furthermore, practical aspects such as storage dimensions and integration strategies are discussed, and the results of this study will be used as basis for decision making with regards to installation of a pilot system.

Keywords: cold thermal energy storage (CTES), PCM, ammonia refrigeration system, Modelica/Dymola modelling

1. INTRODUCTION

Demand for seafood has grown for the last decades and we are annually consuming over 20 kg per capita on a global scale and the number is expected to increase as global fisheries and aquaculture production will play an increasingly important role in providing food (FAO, 2022). Fishery resources are declining due to e.g. overfishing, to which a better utilization and conservation of the landed fish could be a part of the solution. Freezing is a traditional and well-proven conservation method, inhibiting the degradation reactions in the fish so that quality is preserved and shelf life is prolonged, while also allowing for more climate friendly transport methods such as slow, long-going ships. However, as the demand increases so does the energy demand for processing.

Industrial food processing plants have been a study subject for integration of cold thermal energy storages (CTES) the latter years, due to high demand of thermal energy at various temperature levels (-50 to 5 °C on the cold side) and thermal loads that often peaks during high-cost hours (Selvnes et al., 2018; Svendsen et al., 2020). Peak shaving and load shifting are two key features of CTES integration, and storing energy on the demand-side creates a flexibility for both the plant and grid owner. Storing the energy by utilizing the latent heat in phase change materials (PCM) allows for compact design of the storage unit and has many potential applications (Selvnes et al., 2021b). A promising PCM-HEX design is the pillow plate heat exchanger (PPHX) (Joybari et al., 2022), which have been through experimental validation and proven performance at 0 and - 10 °C (Selvnes et al., 2021a).

This paper investigates CTES integration into a pelagic fish processing plant, targeting the batch freezing process taking place at -40 °C, employing industrial-scale PPHX CTES units. Goals of the integration is to reduce electrical peak power demand and generate savings on the energy costs by shifting energy production from high- to low-cost hours.

2. METHODOLOGY

2.1. Case definition

This work is a continuation of the paper by Widell et al. (2022) , in which an energy analysis and potential for CTES integration of a pelagic fish processing plant was evaluated. The plant mainly produces whole (round) or filleted Herring and Mackerel, which is frozen in 20 kg cardboard boxes. Each tunnel has a capacity of 125 tonnes/batch and the process lasts for 22 hours before the fish is frozen (core temperature below -18 °C). In total, the plant has 11 freezing tunnels and 2 refrigeration systems, both employing R717 as refrigerant, but for this case only one of the systems, which covers cooling demand for 5 tunnels and 2 frozen storages, was considered. Nominal cooling capacity of the system is 4 MW (-40/+25 °C), and it has a charge of more than 30 tonnes of refrigerant, which is pump-fed to the evaporators. The energy analysis revealed that the refrigeration systems accounted for about 75% of the total energy consumption (Figure 1).

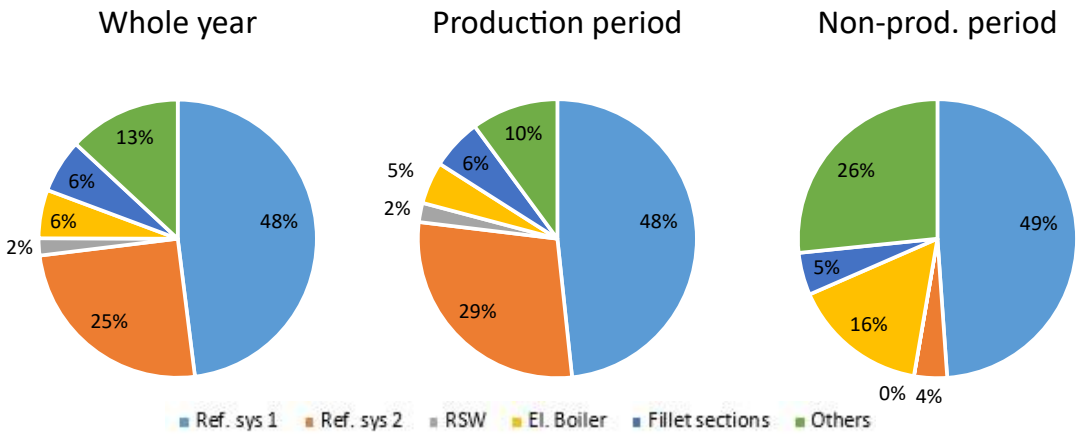

Figure 1: Total energy demand in 2021 for the plant, by sections (Refrigeration systems, RSW system, electrical boiler, fillet sections and others), for whole year and samples from production and non-production periods. From (Widell et al., 2022)

Furthermore, the analysis showed that the electric peak power demand at the plant was about 5-5.5 MW during season (September-February except December), and daily electricity consumptions ranging from 100 MWh to 10 MWh within season. It was assessed that CTES implementation could have benefits for this plant, but that further investigation into detailed design and sizing were required, as well as impact on operational costs and energy savings. This work has now been carried out by two simultaneous approaches: a techno-economic-assessment using an optimization-based python algorithm to dimension the CTES storage based on running costs (Bengsch et al., 2023), and the current paper, more focused on how integration into the

system can be carried out, by building a dynamic model of the refrigeration system in Modelica/Dymola with thermodynamic library components from TILSuite[1].

2.2. Peak analysis

Given the irregularity in the peaks from the operational data, a first step for this work was to determine what constitutes a peak. A script was written in Python to count the number of peaks for a selected period of operational data (see Figure 2), where a peak was defined as:

- having a value of above 3000 kW (X_p)
- minimum 24 hours between each peak
- peak period was determined by traversing left-right from identified peak to nearest point in which the value is close to the cutoff limit y_{cutoff} ($X_1 - X_0$)
- energy in the peak was calculated by integration over the peak period (above cutoff limit)

In addition, the time between peaks was identified, labelled 'charging period'. Further useful insight can be calculated from these parameters: required (average) discharge and charge rates can be calculated by dividing peak energy over the peak period and charging period; maximum discharge rate can be calculated as the difference between peak point value and cutoff-limit. All these parameters give valuable input to the sizing strategy of the CTES.

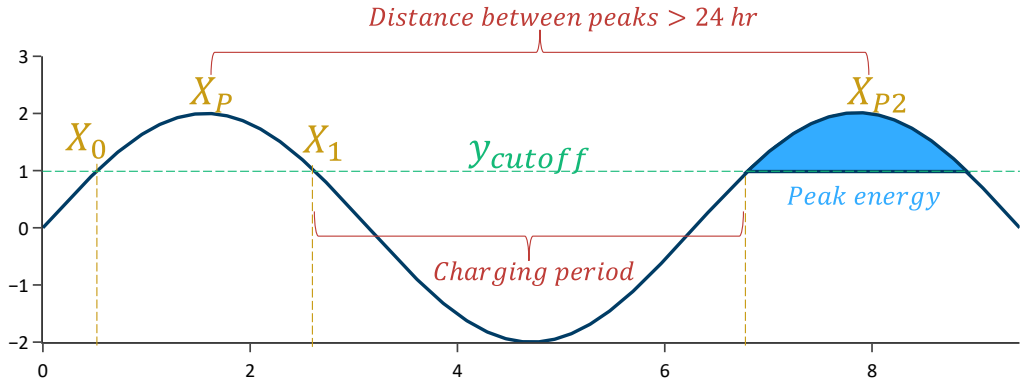

Figure 2: Identification of peaks in operational data

2.3. Concept for CTES integration and simulation model

It was assumed that a temperature difference of minimum 5 K is necessary to facilitate for proper charging and discharging, meaning that a PCM with a melting temperature at maximum -45 °C should be selected. As noted in the previous studies, reliable commercial PCMs at this temperature range are currently scarce, and often the phase change temperature is more a gliding range than a fixed plateau (Joybari et al., 2023; Selvnes et al., 2021b). A modified version of the commercial PCM ATS-40 (Axiotherm GmbH, 2023) was selected with relevant properties listed in Table 1. The phase change temperature was changed to -45 °C and phase change enthalpy was set equivalent to heat storage capacity from the datasheet. Ammonia is not a suitable refrigerant to charge the CTES unit due to high vapor-specific volume at the required temperature level (< - 50°C). Therefore, a separate 'charger circuit' was proposed, employing CO_2 as a refrigerant. CO_2 has more suitable properties at low temperatures and can be operated as a conventional refrigerant above the triple-point (--56.6 °C). However, introducing a second refrigerant also introduces a challenge regarding system integration, since the PPHX plates at its current design only has one internal flow channel.

[1] https://www.tlk-thermo.com/index.php/en/til-suite

Table 1: Properties of PCM used in the model, a modified version of ATS-40

Property	Value
Phase change temperature (°C)	-45
Phase change enthalpy (kJ/kg)	180
Density, (liquid / solid) (kg/m^3)	1450 / 1363
Specific heat capacity, liquid (kJ/kgK)	3
Heat conductivity, both phases (W/mK)	0.6

One possible solution to this is to use an intermediary, pump-circulated heat transfer fluid (HTF) (e.g., CO_2) in combination with some clever pipe-valve work, which transfer heat to-from both the charging circuit and the refrigeration system. This would however also require even lower evaporation level to ensure proper heat transfer from the charging process, and thus increase the power requirement. Another solution, adopted in this work, is a modified PPHX plate design with 2 internal flow channels. Examples of such designs, or 'embossing configurations', has been described by Joybari et al. (2022). It should be noted that the CTES component used in the modelling had only one internal channel for simplicity.

A simplified sketch of how the CTES units could be integrated into the refrigeration system is shown in Figure 3. The black lines represent how the current refrigeration system operates; liquid ammonia is pumped from a separator, overfeeding the evaporators in the freezing tunnels (and also frozen storage) before it returns to the separator. The compressors (represented by one single unit in the drawing) ensure a correct pressure level in this circuit by regulating the filling level of the separator, i.e., it removes and compresses vapour which requires work input. By adding a CTES downstream of the tunnel freezers (red lines in drawing) part of the evaporated refrigerant would condense in the CTES, reducing the amount of vapour the compressors must remove and thus reduce work input. In addition, two 3-way valves would let the ammonia flow through the units while discharging and bypass it during charging, accomplished by a separate CO_2 charger system (blue lines).

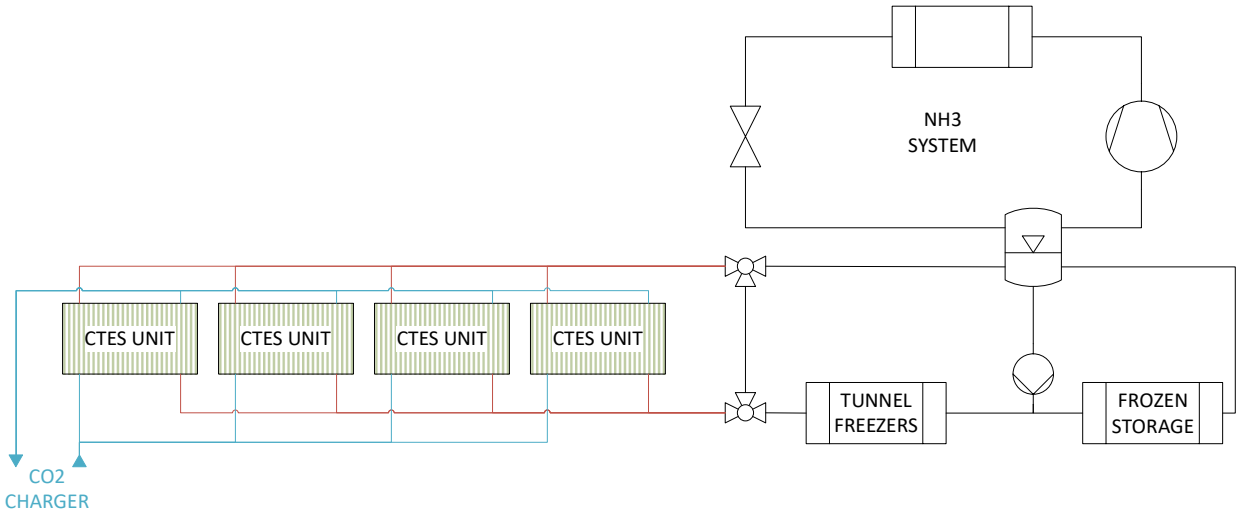

Figure 3: Simplified drawing of proposed CTES integration

Figure 4 shows a snapshot of the model from Modelica. The tunnel freezers are represented by a pipe component (1) with a heat port attached and using a TILFileReader component (2) to feed the model with operational data (i.e., cooling demand for the freezers). A refrigerant pump (3) is used to pump liquid NH_3 from the separator (4) to the tunnels, controlled by a PI controller (5) that regulates on the outlet refrigerant quality after the tunnels. This means that the mass flow through the freezers (and CTES units) is not constant. In the original system the two-phase refrigerant would return to the separator through valve (6). This figure shows the modified system where 4 CTES units (9) are integrated using a valve (7) and two controllers (8) to regulate the flow. To model the CTES units, the TIL PCMStorages Addon has been used, with the

'PillowPlateInBlock' component which was recently validated against experimental data (Försterling et al., 2022) . The following geometry was used: L: 5.5 m, W: 2.2 m, H: 1.8 m. These geometries are restricted by the internal volume available in a 20-foot container, which is a convenient size for a CTES unit. Also note that there is an extra freezing circuit dedicated to the frozen storages (11), which heat load also affect power input to the compressors (10).

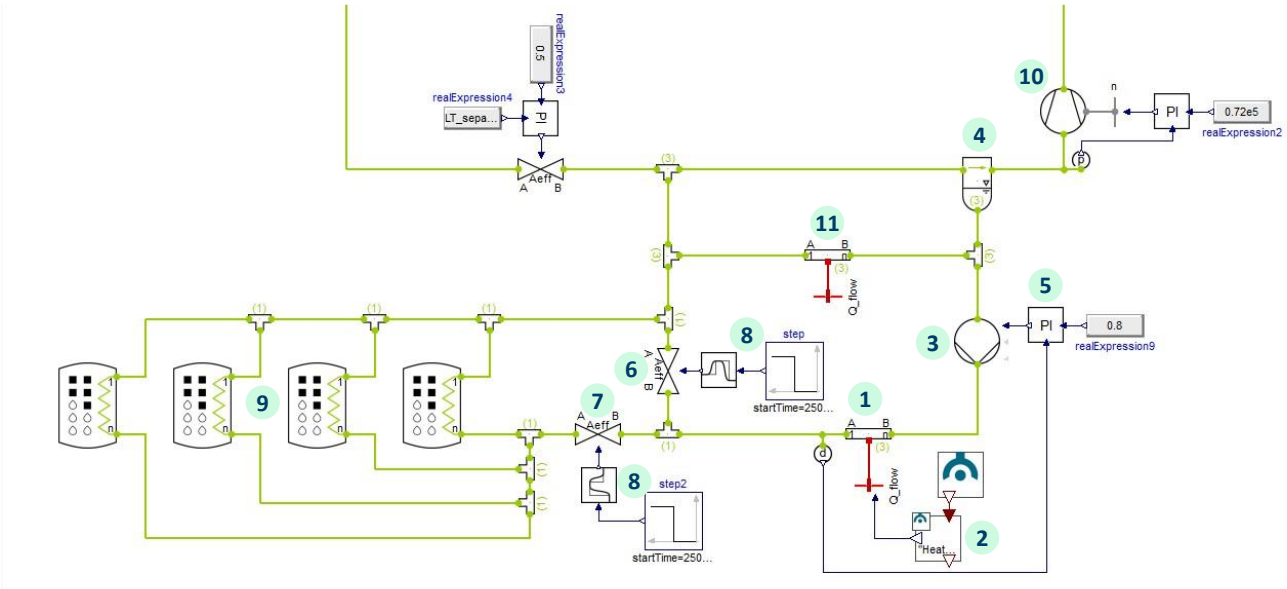

Figure 4: Snapshot from relevant part of the model from Modelica

The CTES units are connected in parallel, and with equal pressure drop the flow is evenly distributed. Number of units can easily be changed by simply removing/adding one component and the attached pipework. Several simulations have been run on this model, with variation in the following parameters to investigate its effects on the overall performance: plate pitch (15, 30 and 45 mm), number of units (1, 2, 3, 4), and discharge strategy (simultaneously and stepwise).

3. RESULTS

3.1. Peak analysis of data

Hourly cooling demand data for the period August to December 2021 was used as input to the peak analysis, constrained by a cutoff limit at 3000 kW. Figure 5 shows two samples from the period for visualization: peaks are marked as green dots surrounded by grey areas indicating the peak duration.

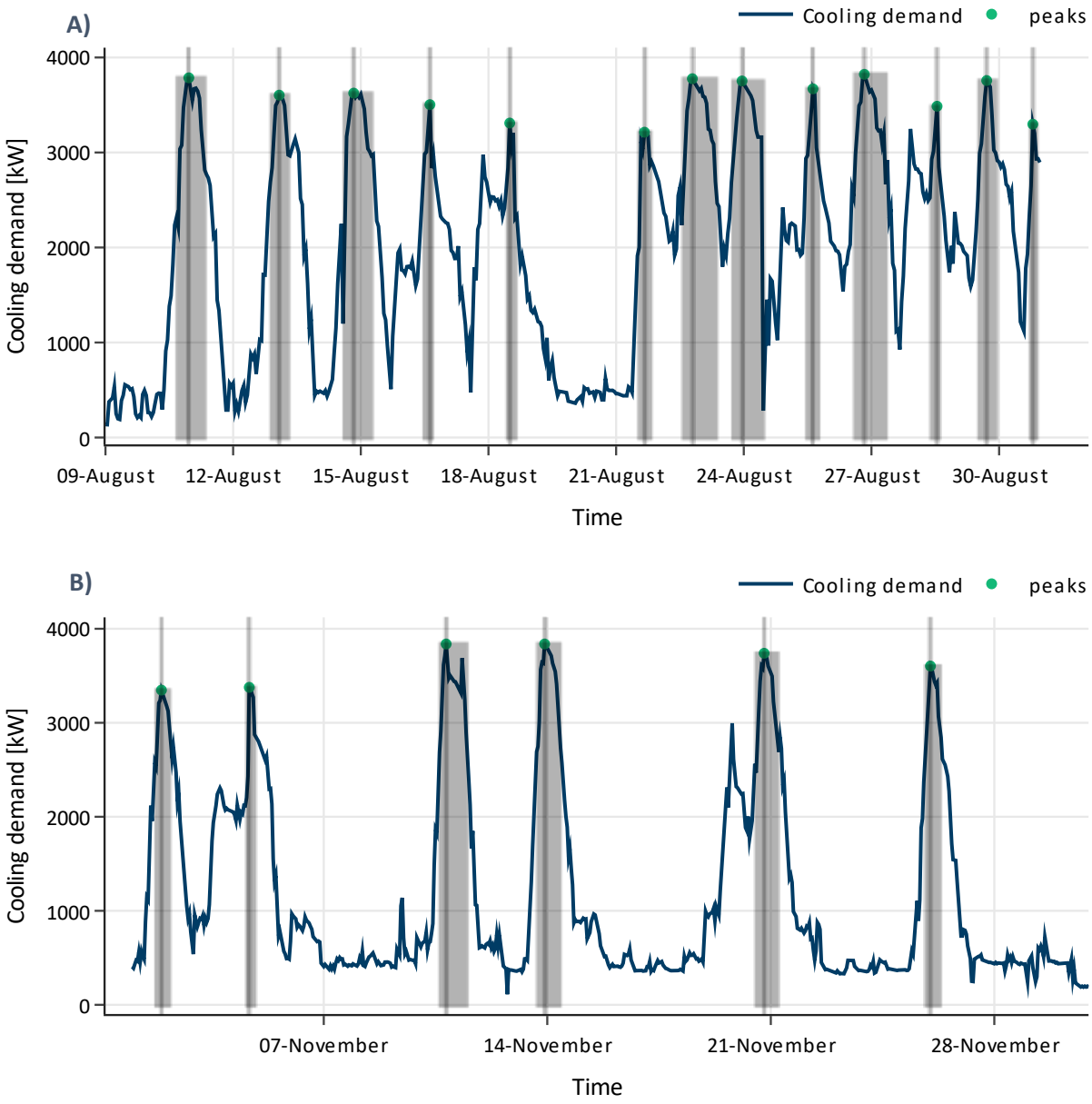

Figure 5: Subsets of cooling demand data with identified peaks. A) 9th to 31st of August, B) November

In total, 37 peaks were identified for the entire period, with an average peak value of almost 3600 kW and duration ranging from 3 to 19 hours. The peak energy is a measure on how much cooling capacity is needed to cover the peak, which is dependent on length of the peak. As seen in Figure 6 many of the peaks are lasting in the range of 14-19 hours, with peak energy content levels from 5000 to 11 000 kWh. These peaks would, on average, require a discharge rate between 342-615 kW, and even higher maximums, if a peak was to be shaven 'perfectly' (i.e., capped at 3000 kW).

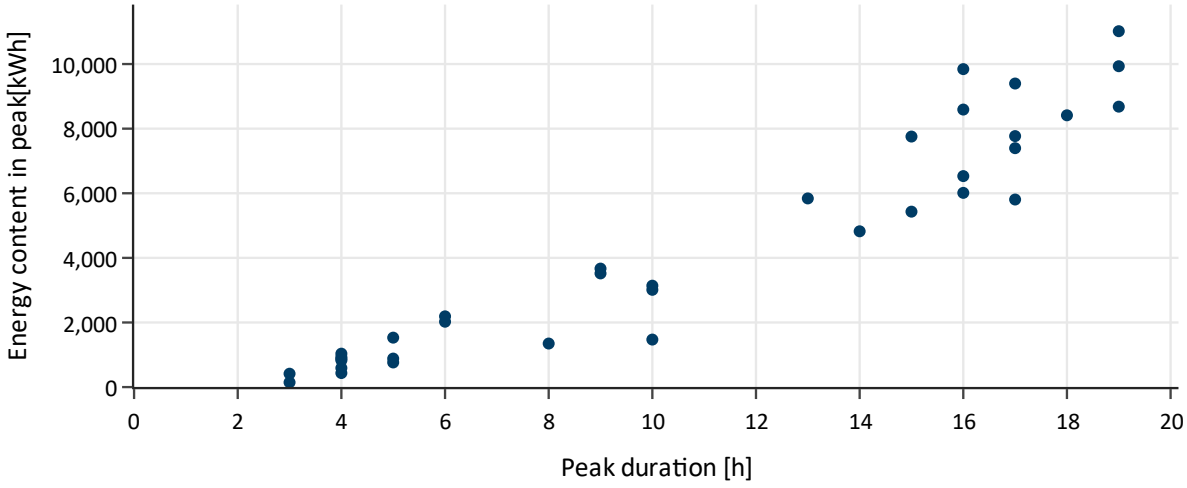

Figure 6: Peak energy content vs peak width (length of peak)

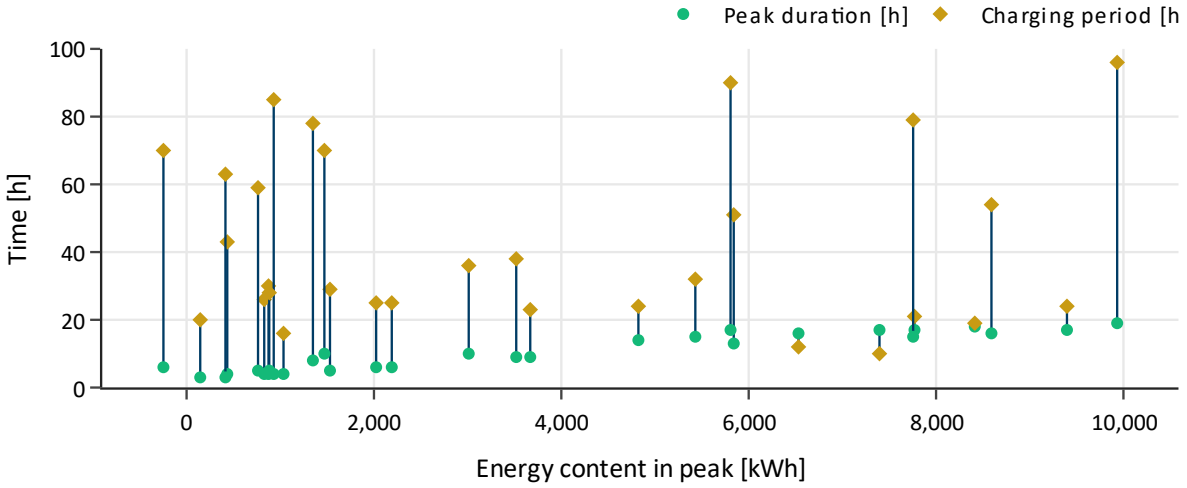

Figure 7: Energy content, length and available time ahead for charging for each peak. Green dots are peak duration, yellow diamonds are charging time available. Peaks where charging period exceeds 100 hours not shown

Figure 7 also shows the available charging time ahead for each peak, which is an important input since charging and discharging of the storage not necessarily have to occur at the same rate. Increased charging rates could be accomplished with large temperature differences between the PCM and charging fluid (CO_2), but would also lead to reduced evaporation pressure and thus more work input to the CO_2 compressors in order to charge. For this case, the result reveals that the available charging periods is longer than the following peak periods for almost every peak, i.e., increased charging rates are not necessary. However, this is not always the case, meaning that for a storage to be able to shave every peak, it must be sized for the 'worst case'.

3.2. Effect of different plate pitches

The distance between plates, or plate pitch, is an important parameter that influences storage capacity, i.e. the volume available for PCM and thus capacity. A large pitch leaves more room for PCM and more storage capacity. A smaller pitch leaves less room for PCM, but at the same time allows more plates to be installed within the storage vessel, which in turn increases the heat exchange area and the achievable charge/discharge rates. This phenomenon was tested before CTES integration in the simulation model for three different configurations, as listed in the Table 2, with the discharge rate over time plotted in Figure 8.

Table 2: Selected properties for different plate pitch configurations

Property	$\delta_0 = 15\ mm$	$\delta_0 = 30\ mm$	$\delta_0 = 45\ mm$
PCM volume [m^3]	16.5	18.9	19.7
Storage capacity [kWh]	1160	1369	1449
Number of plates	106	56	38

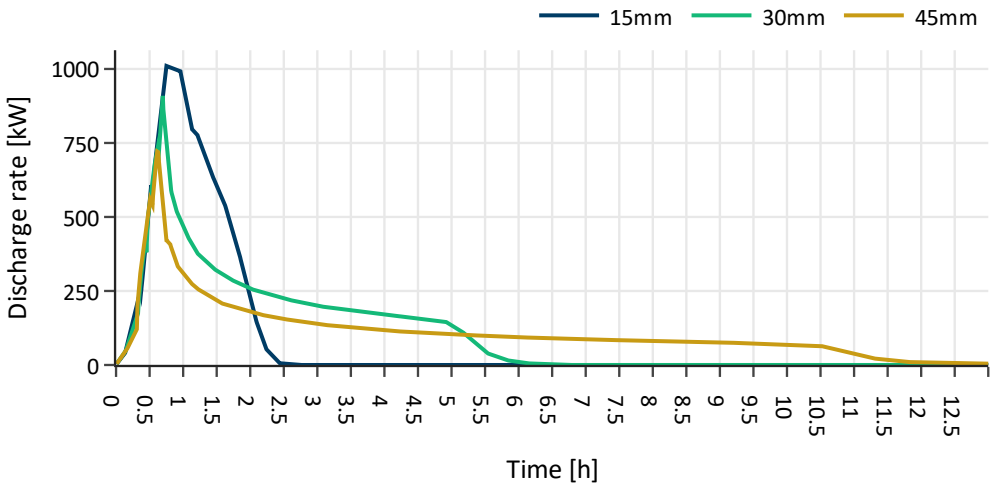

Figure 8: Discharge rate for different plate pitch configurations

As can be seen, a pitch of 15 mm gives the smallest capacity because of a high plate density, but also gives a sharp and high, but short-lasting discharge rate which can be effective when targeting tall-narrow peaks. Using a 45 mm pitch increases capacity by almost 25%, but simultaneously gives a smaller discharge rate over an extended period. In numbers, the 15 mm case gives a maximum and average discharge rate of 1010 and 444 kW, 30 mm gives 909 and 206 kW and 45 mm gives 721 and 108 kW. Note that HTF flow through the unit for these cases were unregulated which impacts the results, i.e., the mass flow increased during the first 3 hours.

3.3. Cascading of CTES units

To investigate the effects of cascading several units into the system, a plate pitch of 30 mm was selected, as it represents a balanced course between capacity and discharge rates This gave each storage a capacity of 1369 kWh and a maximum and average discharge rate of 909 and 206 kW, respectively. One peak from the operational data profile was selected as simulation period, i.e., a 33-hour window of cooling demand (see 'Cooling load' in Figure 9). For the first set of simulations, the discharge from all units was controlled to start simultaneously.

Figure 9 (top) shows the (combined) discharge rates for the cases where discharging was set off simultaneously, and it can be seen that both maximum and average discharge rates elevate as we add more units into the system. For these cases, the units were set to discharge right before the 7-hour mark, using a simple time controller to open the valve(s) in front of the units. The bottom graph in Figure 9 shows the impact on the electrical power demand of the compressors, and the characteristics of the discharge rates transfers onto these curves: an initial, sharp drop followed by a sharp increase, before the curves gradually converges to base case values as the storage capacity is drained. In terms of energy consumption, reductions of 2.3%, 4.3%, 6.3% and 8.0% (1700-5900 kWh_{el}) were observed. Peak power reduction was rather poor however, reducing the base case value by 0.7%, 1.3%, 1.7% and 2.1% (22 – 70 kW). This is partly due to mismatch between the initialisation of the units and the cooling demand, and partly due to the discharge characteristic. The discharge period lasts about 6-6.5 hours before the units are discharged, and we see in the graphs that the end of the discharge periods occurs almost at the same time the cooling demand peaks.

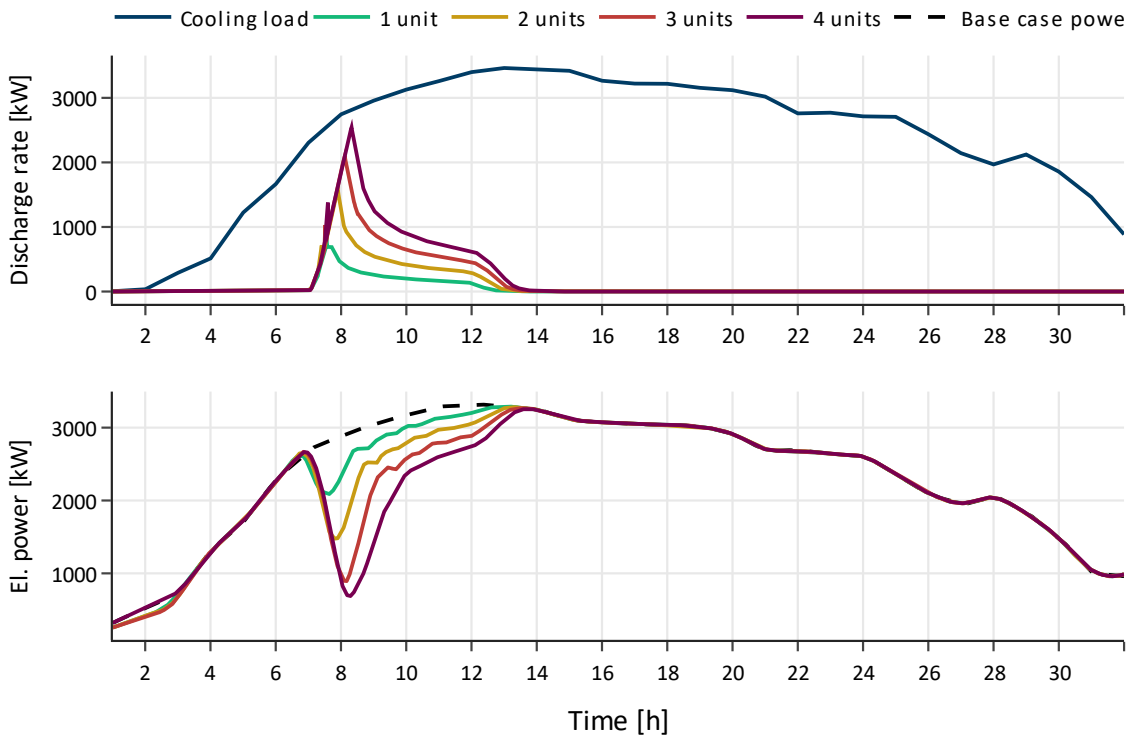

Figure 9: Discharge rates and electric power demand of the compressors for cases with simultaneous discharging of units. Top: Discharging rates. Bottom: Power demand of compressors.

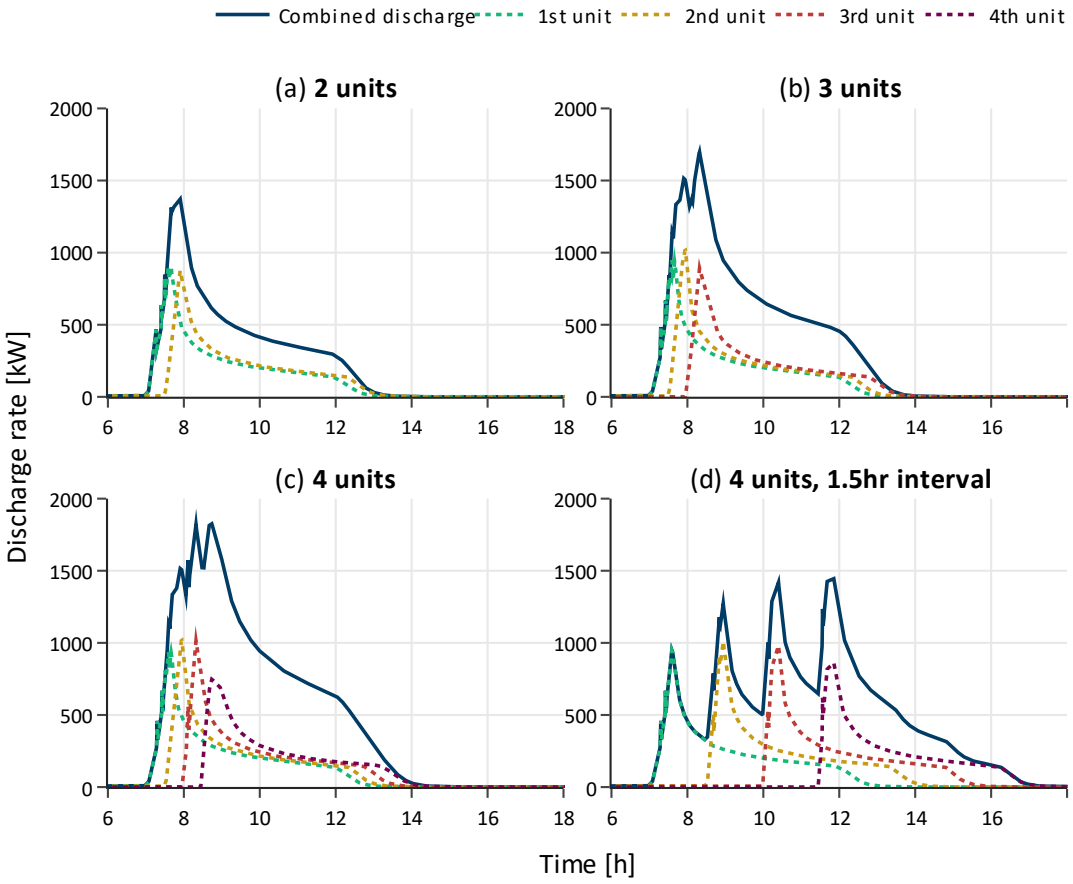

Figure 10: Discharging rates (unit-wise (dots) and combined) for cases with stepwise discharging of units: case (a), (b) and (c): 30 min between discharging starts, (d) 1.5 h between discharging starts

To extend the discharge period, a different timing schedule of units were tested. Figure 10 shows the resulting discharge rates for these cases, where the units were set to discharge with 30 min intervals in between, and one case with 1.5 hour in between. The graphs show the discharge rate per unit and the combined discharge rate per configuration. Compared with the cases where units discharged simultaneously, the periods have now extended from 6-6.5 hours to 6.4-7.33 hours, and 10.2 hours for case (d). Even though the total discharge periods are extended, the characteristics of the curves are not optimal, i.e., too jagged. A different control strategy is needed to better distribute the stored energy over the peak period, likely by controlling mass flow through the units. Furthermore, a reliable method for determining state-of-charge in the units is required as an input parameter for the control strategy.

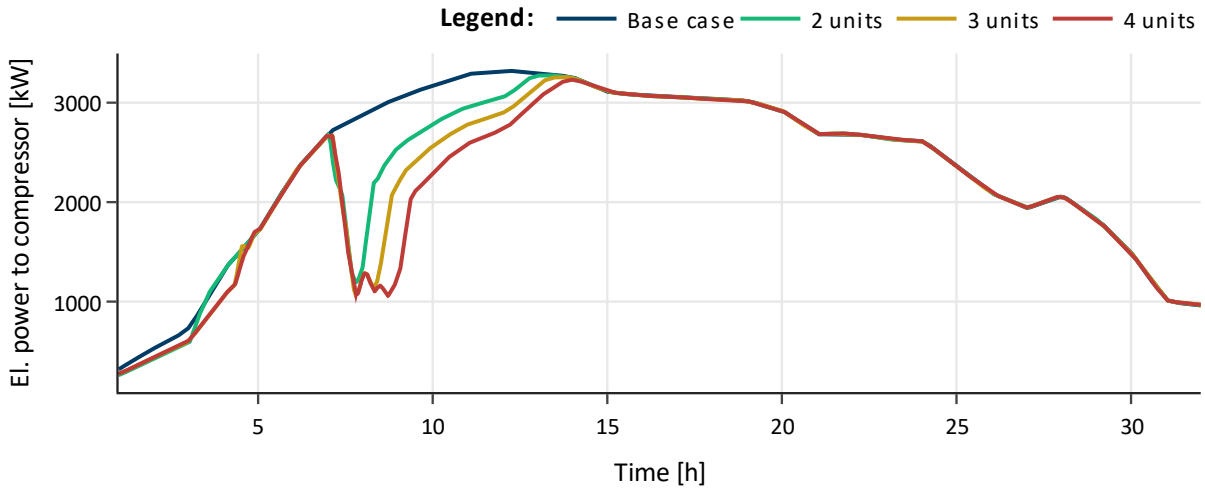

Figure 11: Power demand of compressors for cases with stepwise discharging

Figure 11 shows how the stepwise discharging effects the electrical power demand of the compressors in the system. Note that the case with 1.5-hour interval was not included in these simulations due to the non-favourable discharge curvature seen earlier. Reduction in electrical energy consumption is almost the same, but a bit higher for stepwise discharging, comparing cases with equal number of storages. Since we have been able to further extend the discharge periods, the peak power reduction is also a bit higher, with a maximum of 2.75% for the case with 4 units. Still we see the jaggedness from the discharge rates transfer onto the power curves, which leads to undesired operation of the compressors. Table 3 summarizes selected results for all cases.

Table 3: Selected results from all cases. Numbers 1-4 refers to number of units. 4*: 4 units with 1.5hr interval

	Simultaneous discharge				Stepwise discharge (30 m interval)			
Parameter	**1**	**2**	**3**	**4**	**2**	**3**	**4**	**4***
Discharged energy [kWh]	1370	2848	4322	5772	2857	4315	5749	5781
Peak power reduction [%]	0.66%	1.33%	1.69%	2.12%	1.43%	1.97%	2.75%	n.a.
El. energy reduction [%]	2.27%	4.26%	6.34%	7.99%	4.41%	6.71%	8.73%	n.a.
Discharge period [h]	5.95	6.18	6.35	6.5	6.36	6.84	7.33	10.2
Discharge rate max [kW]	742	1567	2098	2453	1371	1698	1826	1445
Discharge rate, avg. [kW]	230	463	688	896	446	628	781	564

4. DISCUSSION, CONCLUSION AND FURTHER WORK

From the plant owner's perspective, the goal of CTES integration is to reduce the peak power demand and shift cold production from high- to low-cost hours, by targeting the batch freezing process which takes place at -40 °C. Thereby also the maximum power required from the grid can be significantly reduced, reducing the

periodic cost for power provision. A previous study covered an energy analysis of the plant and revealed a potential of CTES integration.

A detailed analysis of the cooling demand was carried out and 37 cooling demand peaks were identified between August and December of 2021 (peak-season), of which many had high energy contents (5000 - 11 000 kWh) and lasted for long periods (14-19 hours). It was also found that there was sufficient time to charge storages ahead of almost every peak.

Discharge simulations with varying plate pitches showed the effect on capacity and heat transfer rate. A 15 mm pitch resulted in high maximum/average discharge rates (1010/444 kW) with (relatively) low storage capacity (1160 kWh), while 45 mm pitch resulted in reduced rates (721/108 kW) and higher capacity (1449 kWh). The 30 mm, chosen for further simulations, represented a balanced course between the former.

The CTES units were in the model integrated downstream of the tunnel freezers in parallel, with valves, pipework and controllers that ensured an evenly distribution of the refrigerant mass flow. Several simulations were carried out using different number of units (1 to 4) and two different discharge strategies (simultaneous and stepwise). For the simultaneous cases, the discharge rate increased as number of units increased, but the discharge period stayed the same (6-6.5 hours). In terms of energy reduction, best case (4 units) resulted in 8% (5900 kWh) of electrical energy saved (compressor work) during the period, while the peak power reduction was only 2.1% (70 kW). To improve the performance, a stepwise discharging strategy was tested. Using an interval of 30 minutes between the start of each unit, the results showed that the discharge period could be increased to 7.3 hours (4 units). However, the discharge curvatures exhibited an undesired jaggedness, which was especially noticeable for the case with 4 units at 1.5 hours interval. Other means of controlling the discharge rates is required to better distribute the storage capacity over the peak periods, likely by controlling mass flow rates through the units. An increased plate pitch (e.g., 45 mm) could also be a better fit for this case.

Some important aspects of the current model need to be restated. (1) This work proposes using a pillow plate with two internal flow channels to facilitate for NH_3 during discharging and CO_2 during charging, but in the selected model environment we are currently restricted to choose a single channel design. This likely influences the reported heat transfer capabilities. (2) The PCM used in the model was a modified version of the ATS-40, i.e., the phase change temperature was changed from -40 to -45 °C. This was done because of scarce availability of commercial PCMs at the desired temperature levels, and further research into low-temperature PCMs is a necessity for the proposed work to be valid. (3) The work presented in this paper only investigated the discharging characteristics. A complete simulation that includes charging is necessary to paint a fair picture of the overall energy performance of the proposed integration. Further work will address the aspects mentioned, in addition to investigate control strategies that better distribute the storage capacity over the peak periods.

ACKNOWLEDGEMENTS

This study was carried out through the research project KSP PCM-STORE (308847) supported by the Research Council of Norway and industry partners. PCM-STORE aims at building knowledge on novel PCM technologies for low-temperature energy storage.

REFERENCES

Axiotherm GmbH, 2023. Axiotherm PCM Products [WWW Document]. URL https://www.axiotherm.de/en/produkte/axiotherm-pcm/ (accessed 2.6.23).

Bengsch, J., Svendsen, E.S., Galteland, O., Widell, K.N., Selvnes, H., Sevault, A., 2023. Dimensioning and techno-economic-assesment of thermal energy storages in the food processing industry using energy load profiles, in: 10th IIR Conference: Ammonia and CO2 Refrigeration Technologies, Ohrid.

FAO, 2022. WORLD FISHERIES AND AQUACULTURE THE STATE OF. Rome. https://doi.org/10.4060/cc0461en

Försterling, S., Selvnes, H., Sevault, A., 2022. Validation of a Modelica numerical model for pillow plate heat exchangers using phase change material. https://doi.org/10.18462/iir.gl2022.48

Joybari, M.M., Selvnes, H., Sevault, A., Hafner, A., 2022. Potentials and challenges for pillow-plate heat exchangers: State-of-the-art review. Appl Therm Eng 214, 118739. https://doi.org/10.1016/J.APPLTHERMALENG.2022.118739

Joybari, M.M., Selvnes, H., Vingelsgård, E., Sevault, A., Hafner, A., 2023. Parametric study of low-temperature thermal energy storage using carbon dioxide as the phase change material in pillow plate heat exchangers. Appl Therm Eng 221, 119796. https://doi.org/10.1016/J.APPLTHERMALENG.2022.119796

Selvnes, H., Allouche, Y., Hafner, A., 2021a. Experimental characterisation of a cold thermal energy storage unit with a pillow-plate heat exchanger design. Appl Therm Eng 199, 117507. https://doi.org/10.1016/J.APPLTHERMALENG.2021.117507

Selvnes, H., Allouche, Y., Manescu, R.I., Hafner, A., 2021b. Review on cold thermal energy storage applied to refrigeration systems using phase change materials. Thermal Science and Engineering Progress 22, 100807. https://doi.org/10.1016/J.TSEP.2020.100807

Selvnes, H., Hafner, A., Kauko, H., 2018. Cold thermal energy storage integration in a large industrial refrigeration system. Refrigeration Science and Technology 2018-June, 1231–1238. https://doi.org/10.18462/iir.gl.2018.1383

Svendsen, E.S., Hafner, A., Selvnes, H., Widell, K.N., 2020. Energy flow analysis of a poultry processing plant., in: 14th IIR-Gustav Lorentzen Conference on Natural Refrigerants (GL2020). Proceedings. Kyoto, Japan, December 7-9th 2020. International Institute of Refrigeration, pp. 13–18. https://doi.org/10.18462/IIR.GL.2020.1110

Widell, K.N., Svendsen, E.S., Selvnes, H., Sevault, A., Hafner, A., Ståle NORDTVEDT, T., 2022. Energy flow analysis of an industrial ammonia refrigeration system and potential for a cold thermal energy storage, in: 15th IIR-Gustav Lorentzen Conference on Natural Refrigerants (GL2022). Proceedings. Trondheim, Norway, June 13-15th June 2022. https://doi.org/http://dx.doi.org/10.18462/iir.gl2022.0034